# An experimental study on pseudoelasticity of a NiTi-based damper for civil applications

Adelaide Nespoli(1), Enrico Bassani(1), Davide Della Torre(2), Riccardo Donnini (2), Elena Villa(1), Francesca Passaretti(1)

1: Consiglio Nazionale delle Ricerche – Istituto di Chimica della Materia Condensata e di Tecnologie per l'Energia, CNR-ICMATE, via G. Previati 1/E 23900 Lecco (Italy)
2: Consiglio Nazionale delle Ricerche – Istituto di Chimica della Materia Condensata e di Tecnologie per l'Energia, CNR-ICMATE, via Via R. Cozzi 53 - 20125 Milano (Italy)

Corresponding Author:
Adelaide Nespoli
via G. Previati 1/E 23900 Lecco (Italy)
e-mail: adelaide.nespoli@cnr.it
phone:+39 0341 2350 107

**Abstract**

In this work, a pseudoelastic damper composed by NiTi wires is tested at 0.5, 1 and 2Hz for 1000 mechanical cycles. The damping performances were evaluated by three key parameters: the damping capacity, the dissipated energy per cycle and the maximum force. During testing, the temperature of the pseudoelastic elements was registered as well. Results show that the damper assures a bi-directional motion throughout the 1000 cycles together with the maintenance of the recentering. It was observed a stabilization process in the first 50 mechanical cycles, where the key parameters reach stable values; in particular it was found that the damping capacity and the dissipated energy both decrease with frequency. Besides, the mean temperature of the pseudoleastic elements reaches a stable value during tests and confirms the different response of the pseudoelastic wires accordingly with the specific length and stain. Finally, interesting thermal effects were observed at 1 and 2Hz: at these frequencies and at high strains, the maximum force increases but the temperature of the NiTi wire decreases being in contraddiction with the Clausius-Clapeyron law.

**Keyword**

Damper, pseudoelasticity, mechanical cyclic, damping capacity, dissipated energy

## 1. Introduction

In its parent (austenite) phase, a shape memory alloy material shows pseudoelasticity that consists in a non-linear hysteretic mechanical response together with the recovery of large deformations at constant stress [1]. In the stress-strain field, during an isothermal deformation, a pseudoelastic material goes through a first order phase transition from an ordered structure, austenite, to a more deformable phase, martensite. This transition is induced by stress and it follows a well-defined path: during loading, the material firstly goes into an elastic deformation of the austenite phase and then it transforms into martensite at constant stress (stress-induced martensite, SIM). Here, the near-zero stress slope is used to cut through the load during high changes of strain. It is important to underline that the SIM is thermodynamically unstable. Therefore, during unloading it re-transforms into austenite following a path at stresses lower than that of the loading one. As a result, the loading/unloading path shows a hysteretic mechanical trend useful in dissipating a large amount of energy together with the softening of the strain recovery [2]. Additionally, a pseudoelastic material is also able to limit the transmission of forces and to allow the re-centering when it is coupled to a proper mass. All these capabilities best suit damping applications as seismic oscillations [3-7]; in this context, the pseudoelastic component mitigates the ground structure displacement with the control and the recovery of the deformation imposed by the external events.

The use of pseudoelasticity to damp the structural vibrations during a seismic event is addressed in many research works, and a significant number of new base isolation systems as well as new pseudoelastic dampers have been proposed. Huang *et al.* [8] presented a base isolation system composed by two superelastic SMA helical springs and a linear slider; Qian *et al.* [9 and 10] presented two dampers, one composed by pre-tensioned superelastic shape memory alloy wires with friction device, and the other by pairs of NiTi wires to allow the re-centering; Branco et al. [11] studied a superelastic dampers based on NiTi wires installed to strengthen a composite timber-masonry wall; Parulekar et al. [12] design a two concentric pipes, which move mutually thanks to pseudoelastic NiTi wires; Fang et al. and Rofooei et al. [13 and 14] presented new pseudoelastic connections; Kuang et al. [15] embedded SMA wires to promote the self-healing of concrete; Dolce et al. [16] proposed a re-centering damper made of groups of NiTi wires.

The pseudoelastic damping is mainly influenced by two main factors [17]: the first concerns the thermomechanical treatment of the production process. In fact, by working on the temperature and the duration of the heat treatment, a certain change in damping is achievable. As an example, Figure 1 shows that the increase of the temperature and time of the thermal treatment of the preparation process, allows lower austenite elastic modulus; moreover, the stress-induced martensite (loading stress plateau) starts to nucleate at lower stresses and in addition, the mechanical hysteresis becomes higher.

A second way to modify the pseudoelastic response is to change the temperature of the application in accordance with the well-known Clausius-Clapeyron relationship:

$$\frac{d\sigma}{dT} = -\frac{\rho\Delta S}{\varepsilon_t} = -\frac{\rho\Delta H}{T_0\varepsilon_t} \quad (1)$$

where ρ is the density of the transforming element, $T_0$ is the room temperature, ΔS and ΔH the entropy and the enthalpy change of the transformation and $\varepsilon_t$ is the linear strain of the transformation in the direction of the uniaxial stress. Given that all these parameters are constants for a given transformation system, it is commonly regarded that the slope of the linearity, i.e. dσ/dT, is a transformation constant [18]. Figure 2 well depicts the Clausius-Clapeyron phenomenon: the increase of room temperature produces a marked shift of the stresses of the loading and unloading plateau; besides, a reduction of the mechanical hysteresis is also observable. In practical application, the increase of the room temperature turns into a change of season. Therefore, the pseudoelastic mechanical response of a generic damper is affected by the climatic changes.

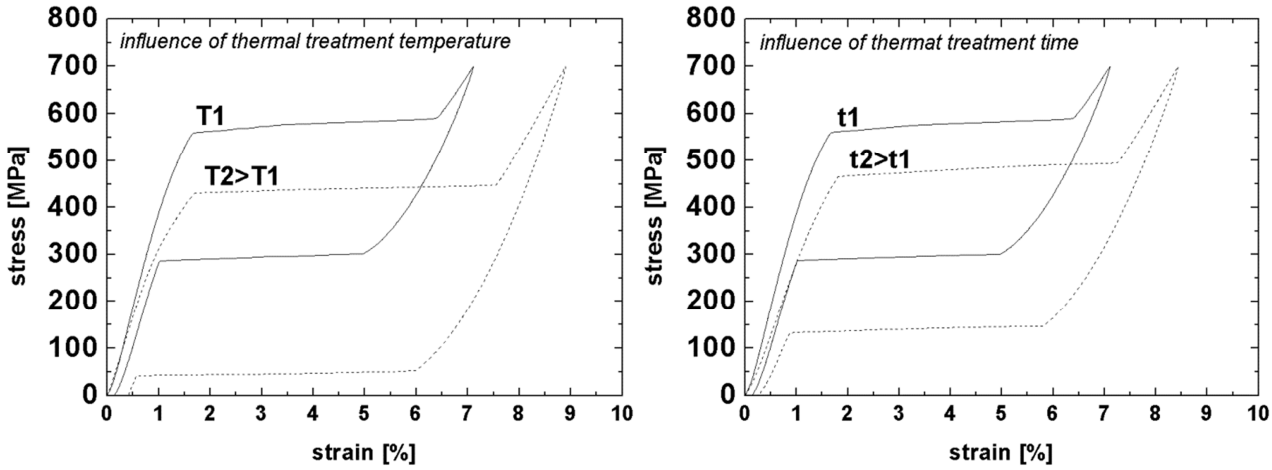


Figure 1. Influence of the thermal treatment temperature and time on the damping response of a NiTi pseudoelastic material. T1 = 300℃; T2 = 400℃ ; t1 = 5 min; t2 = 10 min (Af: austenite finish temperature).

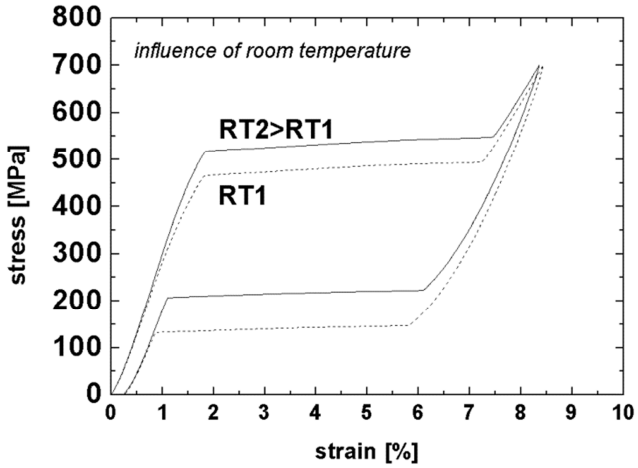


Figure 2. Influence of the room temperature (RT) on the pseudoelastic response of a NiTi wire: RT1 = Af + 10℃, RT2 = Af + 20℃ (Af: austenite fin ish temperature).

Mechanical changes due to thermal effects also occur at high strain rate and with sinusoidal loads: in both these cases, the exothermic/endothermic forward/reverse phase transition produce local change of temperature [19-21]. From the microscopic point of view, these thermal effects rise from the moving austenite/martensite interfaces, each acting as heat source [22, 23]. In this condition, two main effects should be taken into account: first, the temperature of the specimen differs from the ambient one; secondly, the heat transfer equation should take into account both the latent (released/absorbed) and convection heats [24].

As concerns civil applications, Torra et *al.* [7] defined appropriate requirements of a pseudoelastic damper. As regards the mitigation of the oscillations in structures induced by a seismic event, they reported that the device has to work at least 1000 working cycle with an oscillation frequency up to 1 Hz. In accordance with Torra's requirements, this paper addresses the damper proposed in [2] and studies its damping properties together with the thermal effects during testing up to 2Hz of working frequency and for 1000 working cycles.

## 2. Experimental

This work studies the mechanical response at different working frequencies of the complex damper described in [2] and reported in the photograph of Figure 3. The device is composed by two groups of pseudoelastic NiTi wires with identical diameter (1.2mm). Each group includes four NiTi wires with different length (210 and 132mm) in two-pair parallel configuration. The two groups are specularly mounted one with the other to allow re-centering and a bi-directional motion of the damper.

Mechanical tests were performed via a servo-hydraulic machine (MTS 810, with a static/dynamic capacity of 100kN) in tensile/compressive mode at 25-27℃; the device was tested at 0.5Hz,1Hz and 2Hz for 1000 working cycles at a maximum displacement of ±8.4mm. At this deformation, the 210mm long wires work at a nominal 4% strain, whilst the 132mm long ones work at a nominal 6.4% strain. Each NiTi wire was pre-loaded at approximately 48MPa and the device underwent to a low-rate stabilization cyclic before testing (five mechanical cycles at ±8.4mm with a rate of 1%/min, calculated on the length of the longest wires). During mechanical tests, the local temperature of a long and a short wire was measured through thin K-type thermocouples connected to an Eurotherm data logger. The thermocouples were wrapped with Teflon tapes around the NiTi wires; the mean temperature of each NiTi wire was calculated from the signals registered by three thermocouples positioned in the middle and near the two ends of each wire. Due to the limitations of the device used in these aquisitions, the registrations of the temperature were possible only during the tests at 0.5 and 1Hz.

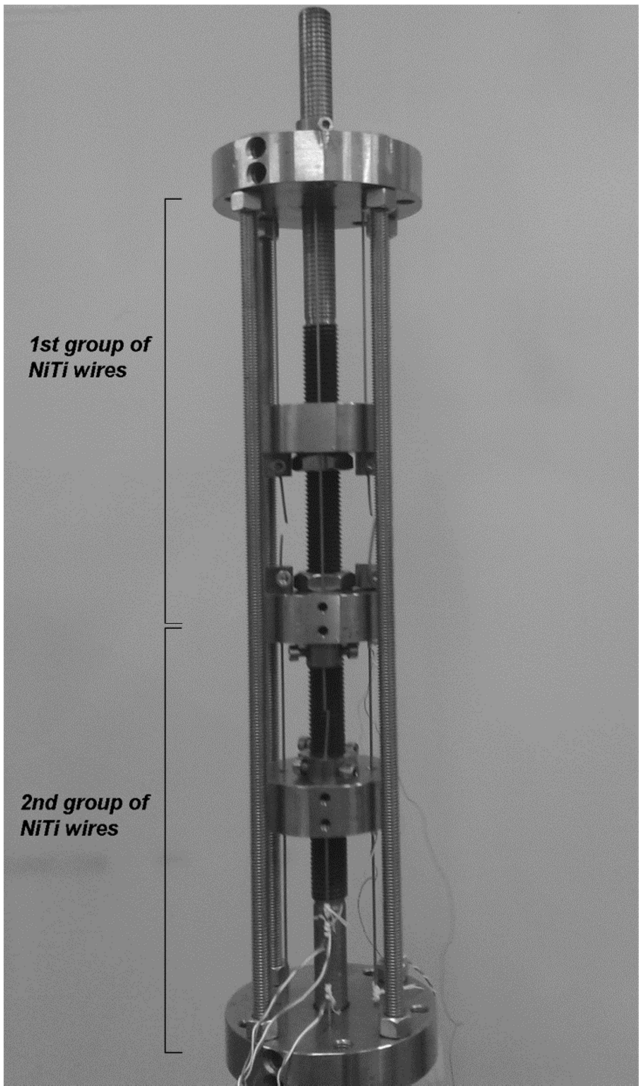


Figure 3. Photograph of the damper [2].

It is worth noting that all the working frequencies considered in the mechanical tests (0.5, 1 and 2Hz) refer to the damper; as previously reported, the damper comprises two groups of NiTi wires that alternately work to assure the bi-directional motion. Therefore, if $f$ is the working frequency of the damper then each group of NiTi wires works at the same $f$ frequency, but it is active for a period that is half the one of the damper $\left(\frac{1}{2f}\right)$. In this period, the NiTi wires of the active group are stretched (loading path) until the absolute maximum deformation (8.4mm), and then they return to the zero strain condition during unloading. After that, they rest for a period of $\frac{1}{2f}$, in which the NiTi wires of the second group become active. Figure 4 and Table 1 report a schematization of the functioning period and the main working parameters of the damper and of a generic NiTi wire that works in the damper.

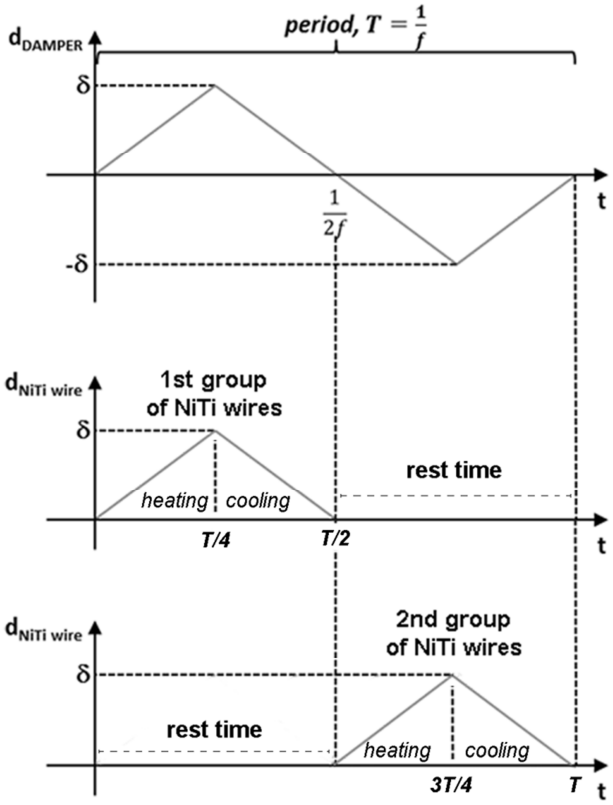


Figure 4. Schematization of a generic working cycle (displacement *vs.* time) of the damper and of the NiTi wires of the first and second groups (working period of the damper: T).

| | damper | NiTi wire |
|---|---|---|
| **stroke [mm]** | ±8.4 | 8.4 |
| **effective working period at 0.5Hz [s]** | 2 | 1 (1) |
| **effective working period at 1Hz [s]** | 1 | 0.5 (0.5) |
| **effective working period at 2Hz [s]** | 0.5 | 0.25 (0.25) |

Table 1. Working data of the damper and of each single NiTi wire that works in the damper; in brackets is the rest period of the NiTi wire.

The key parameters used to evaluate the mechanical performance at a fixed frequency were the dissipated energy per cycle (W), the maximum loading force ($F_{max}$), and the damping capacity (η). Considering a generic mechanical cycle, η was evaluated by the following equation [25]:

$$\eta = \frac{W}{2\pi W_{loading}} \tag{2}$$

where $W_{loading}$ is the mechanical energy stored during the loading path and defined as:

$$W_{loading} = \int_{x1}^{x2} \sigma_{loading}(x)\, S_0 dx \tag{3}$$

and $W$ is calculated as:

$$W = W_{loading} - \int_{x2}^{x1} \sigma_{unloading}(x) S_0 dx \tag{4}$$

with $S_0$ equal to the NiTi wire cross-section, $x_1$=0 and $x_2$= 8.4mm (see Figure 5).

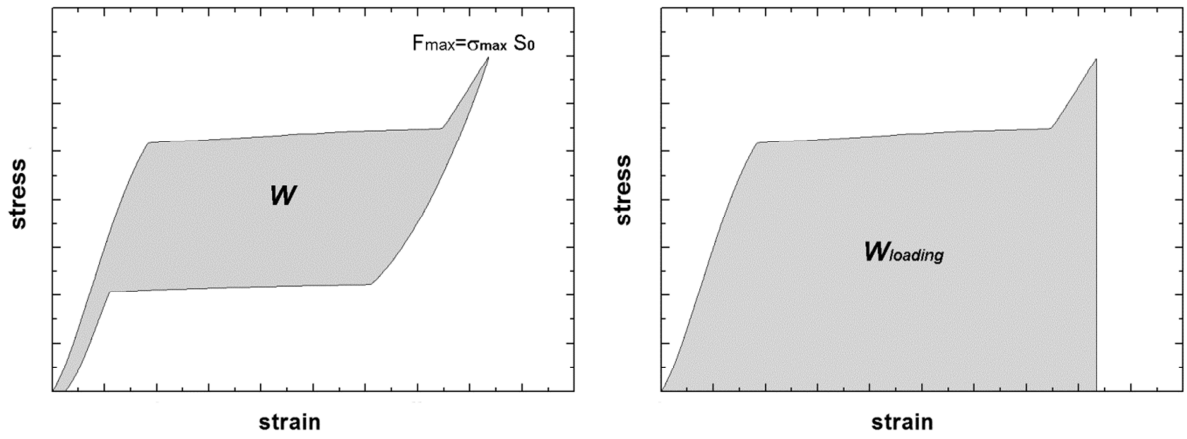


Figure 5. Representation of the dissipated energy per cycle, W, and of the energy stored during the loading path, $W_{loading}$.

## 3. Results

Figure 6 depicts the force *versus* displacement characteristic of the damper during 1000 working cycles registered at 0.5, 1 and 2Hz; the trend of the pseudoelastic curves at the three frequencies is reported in Figure 7. It can be obseved that the device similarly works at 0.5Hz and 1Hz; in particular, it can be seen that at 0.5Hz the damper has a cyclic behaviour that is typical of a pseudoelastic material that works in static conditions [26], with the martesite transformation yield

stress and the SIM plateau that are located at lower stress level and at higher strain values with the increasing of the number of the working cycle.This result is commonly ascribed to the presence of a residual martensite as well as a heterogeneous structure [27] and to a grain reorentation through cyclic tensile loadings [28]. In addition,it can be also observed that the flag-shaped mechanical response at 0.5 and 1Hz changes into leaf-shaped curves after the cycle number 50; the leaf shape is then mantained till the 1000$^{th}$ cycle.The mechanical response at 2Hz quite differes from that registered at the two lower frequencies: the curve at 2Hz has indeed immediately a shape far from a flag, with an almost leaf shape starting from the first mechanical cycle. Even in this case, it is visible a marked change of the pseudoelastic curve starting from the cycle number 50$^{th}$.

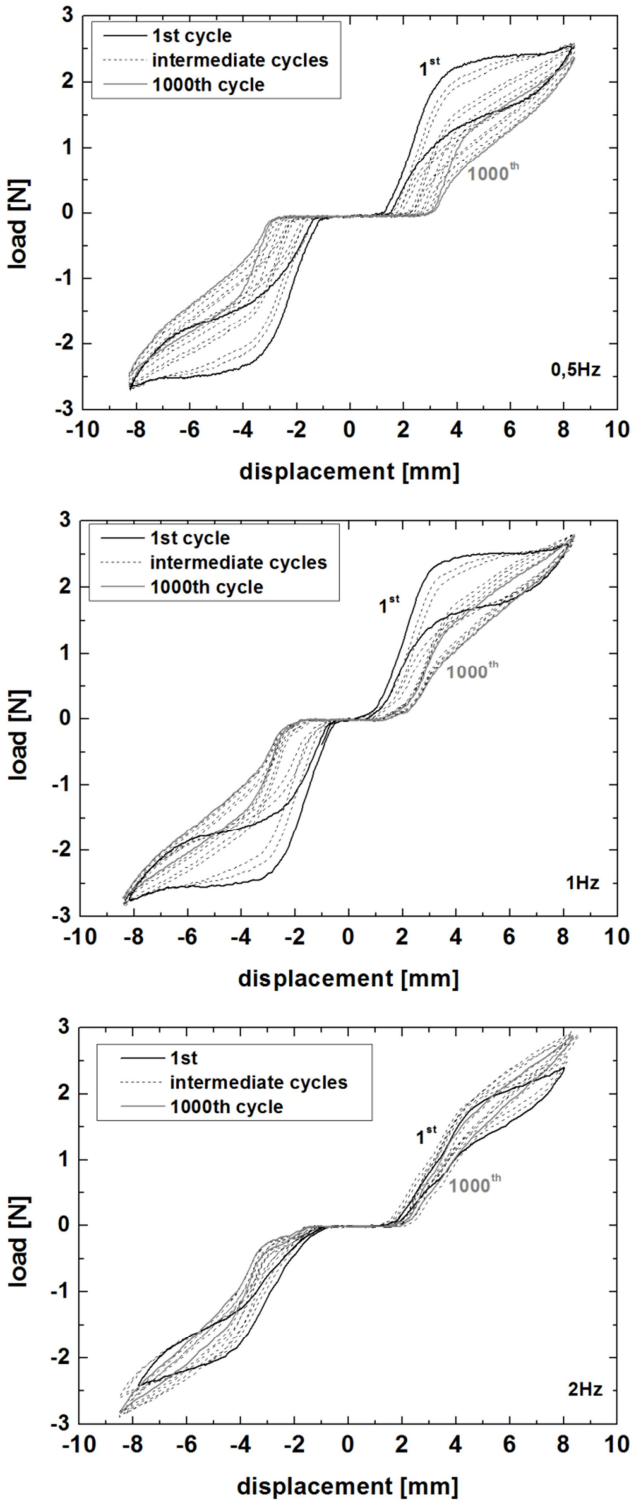


Figure 6. Mechanical tests of the damper at 0.5, 1 and 2Hz; black line: 1st cycle, dark grey line: 1000th cycle, dashed lines: intermediate cycles.

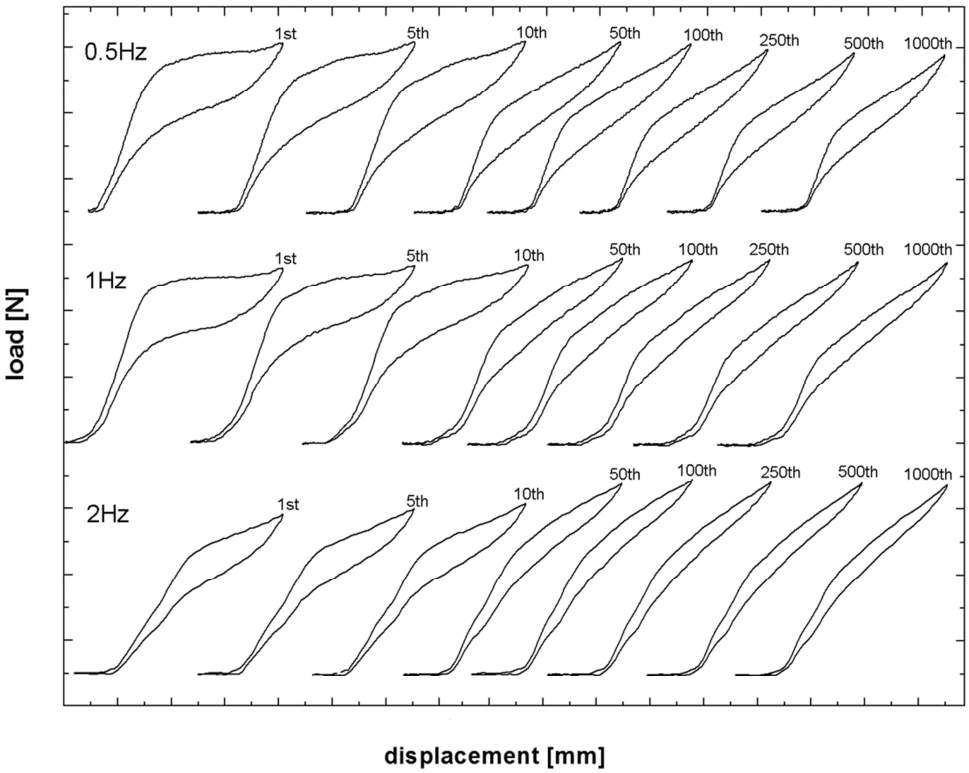


Figure 7. Trend of the pseudoelastic curves at 0.5, 1 and 2Hz.

As a results of the change in shape of the stress induced pseudoelastic curve of the damper there are some evident modifications of the related key parameters, see Figures 8 and 9. It can be particularly seen that the energetic parameters η and the dissipated energy per cycle, considerably decrease with the increasing of the working frequency with a high rate in the first fifty mechanical cycles; after that, the trend becomes almost steady (see Figure 8). At 0.5Hz, η decreases by about 37% and stabilizes at 0.031 while the energy dissipated per cycle diminishes by approximately 50% with a stabilized value of 2.5J. At 1Hz, η decreases by about 38% and stabilizes at 0.027while the energy dissipated per cycle diminishes by approximately 55 % with a stabilized value of1.9J. Finally, at 2Hz, η decreases by about 37.5% and stabilizes at 0.022 while the energy dissipated per cycle reduces by approximately 31% and tends to 1.5J.

On the other side, the maximum force, $F_{max}$, has a double trend depending on the working frequency. At 0.5Hz, $F_{max}$ does not appreciably change with cyclic (it is approximately 2.5kN), while at 1 and 2Hz, it increases throughout the test and tends to 2.8kN and to 2.9kN respectively.

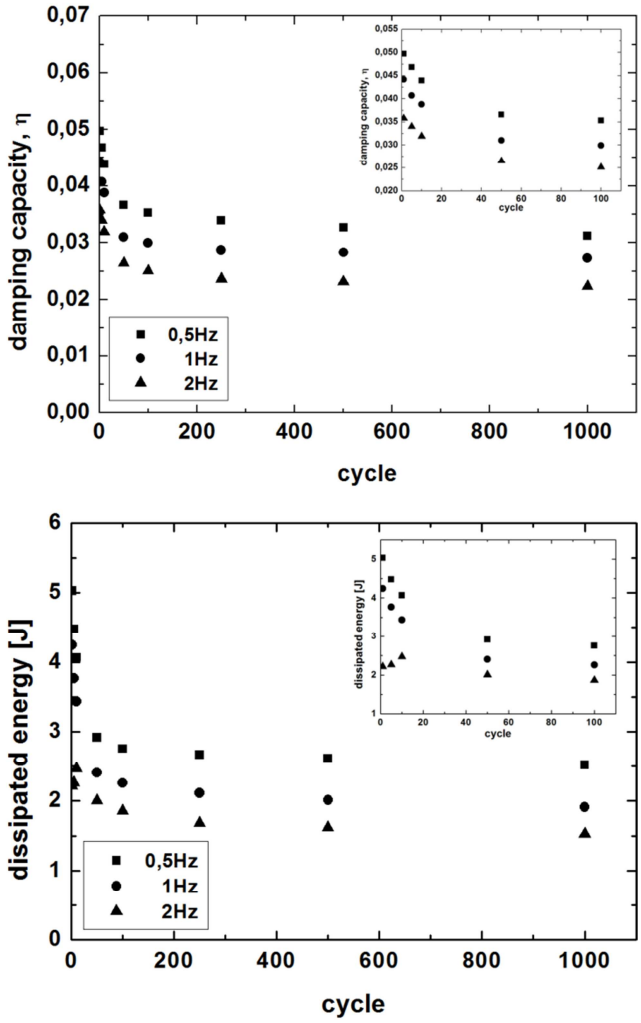


Figure 8. Damping capacity, η, and dissipated energyper cycle of the damper at 0.5, 1, 2Hz as a function of the working cycle. A detailed view of the first 100 cycles is reported in the insets.

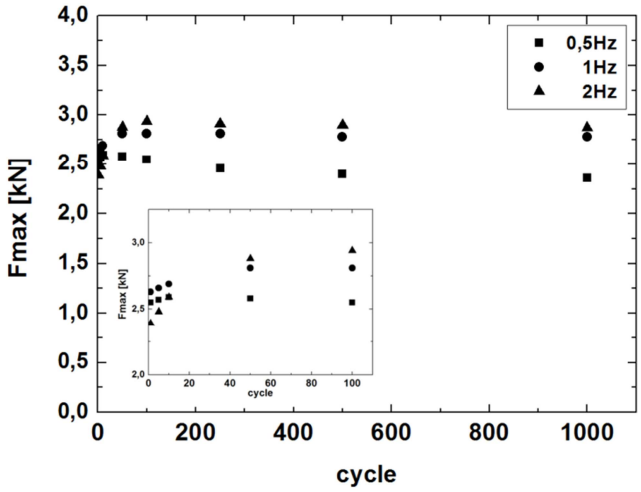


Figure 9. Maximum force of the damper at 0.5, 1, 2Hz as a function of the working cycle. A detailed view of the first 100 cycles is reported in the insets.

Figures 10 and 11 depict the temperature of a short and a long wire of the damper registered during the mechanical tests at 0.5 and 1Hz; the inset graphs report a detail of the first 100 working cycles. As expected, the temperature has a sinusoidal trend (see the detail reported in Figure 12): it increases during the loading path due to the exothermic transition from austenite to SIM, and then it decreases due to the unloading where the endothermic reverse phase transition from SIM to austenite occurs.

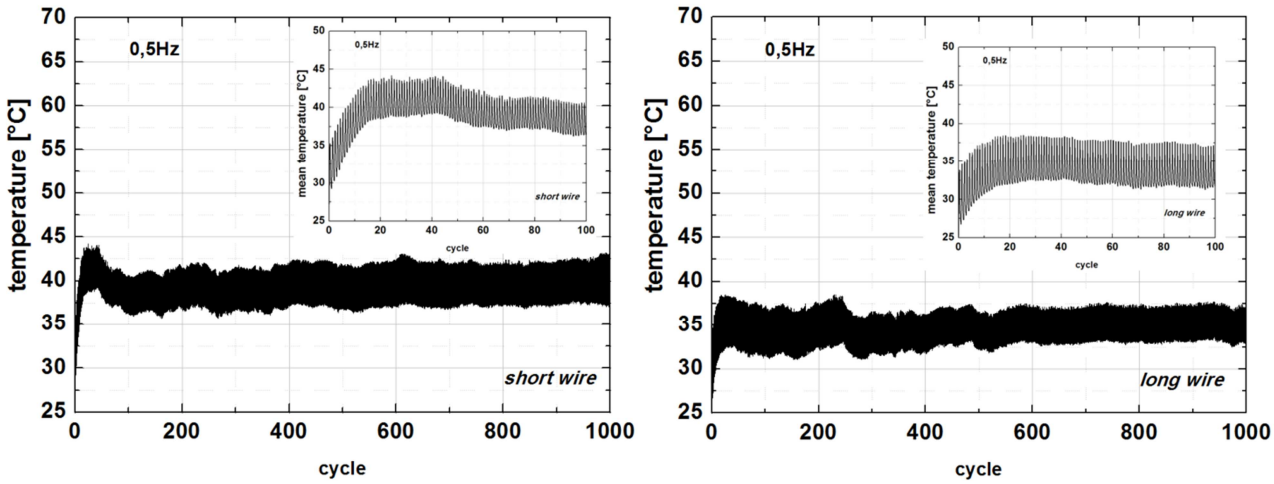


Figure 10. Temperature profile of a short wire, on the left, and a long wire, on the right, registered during 1000 cycles at 0.5Hz.A detailed view of the first 100 cycles is reported in the insets.

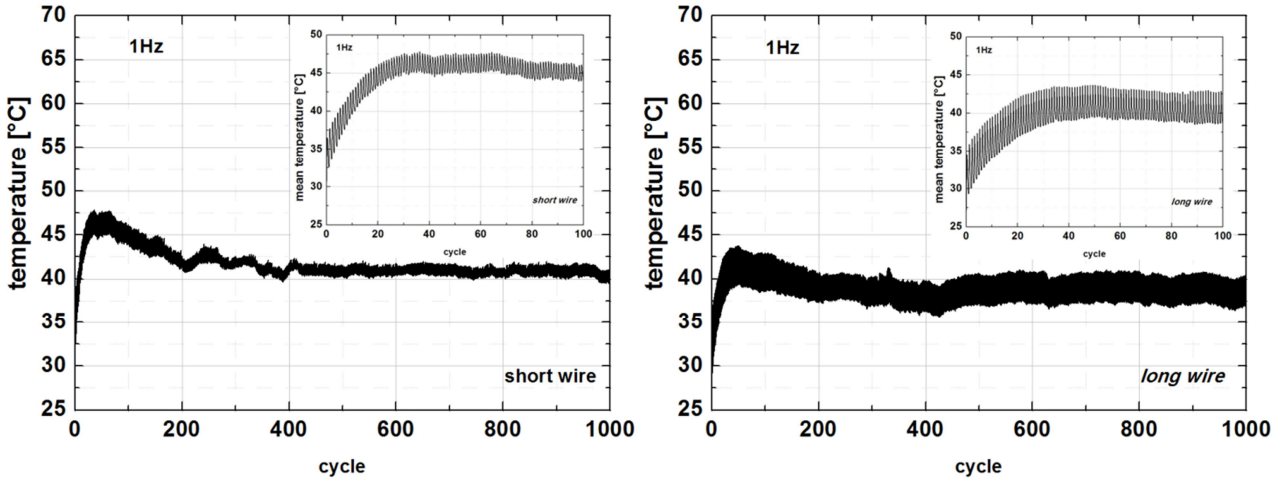


Figure 11. Temperature profile of a short wire, on the left, and a long wire, on the right, registered during 1000 cycles at 1Hz.A detailed view of the first 100 cycles is reported in the insets.

Finally, the use of pseudoelastic curve has recently reached a great interest in the application of elastocaloric effect in solid state refrigeration [29, 30], due to the peculiar thermo-mechanical properties related to the martensitic transition. From this point of view the presented damper can be considered and evaluated also starting form its elastocaloric properties. In this regards, by the measurements of the temperature of the NiTi wires, it is possible to evaluate also the elastocaloric effect of the damper by means of the coefficient of performance (COP) defined as:

$$COP = \frac{\Delta Q}{W} = \frac{\sum m_i C_P \Delta T_i}{W} \quad (4)$$

where m is mass of the NiTi wire (0.96g and 1.5g for the short and long wires respectively) and $C_P$ is the heat capacity (449J/kgK [2]). Figure 12 depicts the coefficient COP of the damper as a function of the mechanical cycle; it can be noticed that the COP at 0.5Hz is higher than that evaluated at 1Hz, and therespective stabilized values are approximately 4 and 3. These COP values, that describes the working efficiency of the pseudoelstic material, are in agreement with those reported in literature [30].

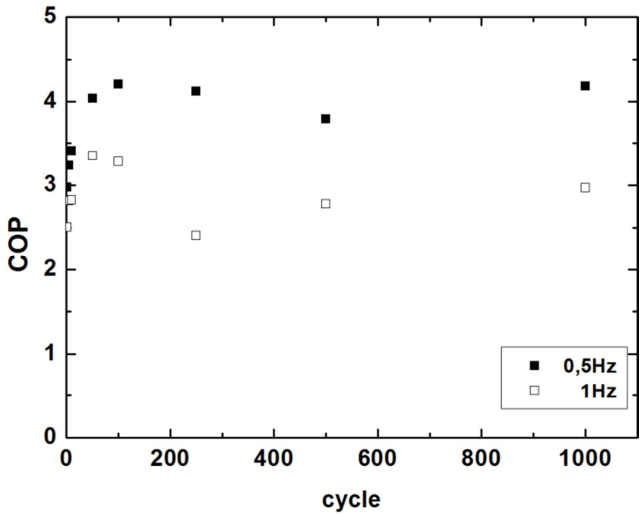


Figure 12. Coefficient of performance (COP) of the damper at 0.5 and 1Hz as a function of the working cycle.

## Discussions

This paper addresses the pseudoelastic damper presented in a previous article [2]; in particular, it refers to the case where the device is composed by two groups of NiTi wires, one working at 4% and the other at 6% of strain.

With respect to the previous work, the present study presents some further experimental tests: the device has been tested at three frequencies (0.5, 1, 2 Hz), for 1000 mechanical cycles. Furthermore, in order to comprehend in deep the mechanical response of the device, the thermal effects on the NiTi components during cyclic were also evaluated.
In particular, the damper is composed by NiTi wires with different length and consequently the shortes wires always reach strains higher than those of the longest ones. This allows the short wires to have a change in the latent heat higher than that of the long wires during the phase transition. With the increasing of the working frequency, the shortes wires are therefore not able to dissipate the heat that is generated during the austenite-martensite exothermic transition and their temperature increases. In fact, in the experimental results it can be seen that the temperature of the short wires is 8-10℃ higher than that of the l ong wires. For the Clausius-Clapeyron relationship, this inevitably allows for an increasing of the maximum force of the short wires and consequently for a global increasing of the maximum force of the damper, see Figure 13.

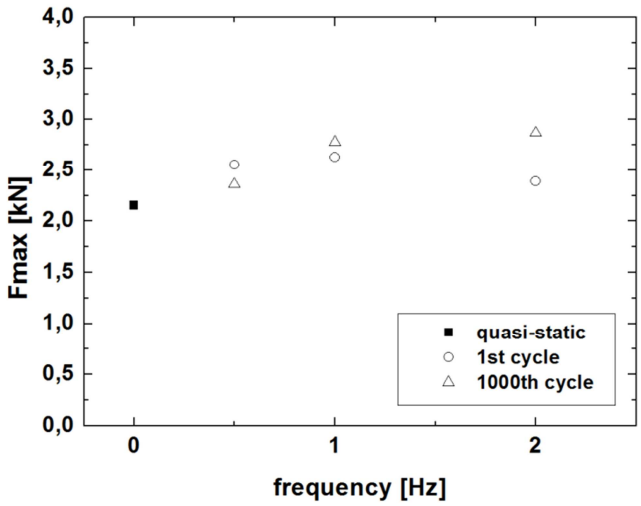


Figure 13. Maximum force *versus* working frequency at the first cycle (round marker) and at the 1000$^{th}$ cycle (traingular marker). The maximum force registered in quasi-static condition is reported as well (square marker).

Figures 8 and 9 show that with the increasing of the working frequency, the energetic parameters (i.e. the damping capacity and the dissipated energy per cycle) decrease with the working frequency; furthermore, they stabilize to values that are lower than that registered in quasi-static condition, see Figure 14. This effect is primarily due to the change in shape of the pseudoelastic curve. This result means that at high frequency we loose at least half of the energetic performance that we can register in a quasi-static tests. This is an important point to fix in mind in the design of a pseudoelastic damper that work at high frequency or at least in a non-static condition.

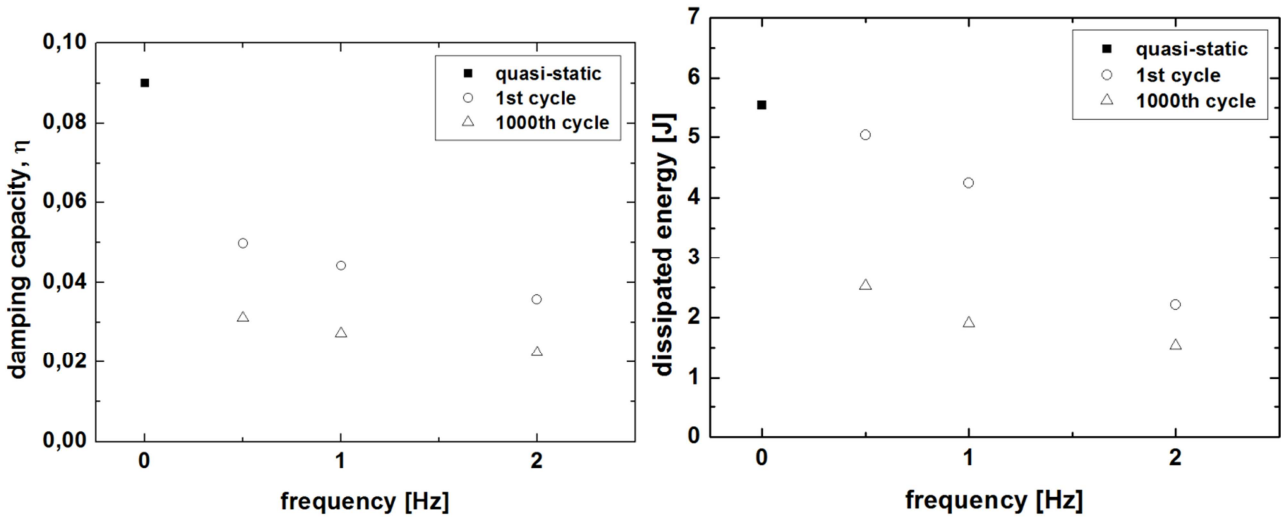


Figure 14. Damping capacity and dissipated energy per cyle versus the working frequency at the first cycle (round marker) and at the 1000$^{th}$ cycle (triangular marker). Data registered in quasi-static condition are reported as well (square marker).

In addition, some significant further results may be highligheted: the first refers to the general trend of the temperatures independetly from the length of the NiTi wire and from the working frequency of the damper. With respect to this feature, in all measurements it can be observed that the temperature cycle increases in the first few mechanical cycles after which there is a sort of relaxation followed by the achieving of a thermodynamic equilibrium with the surround. It means that in the first 50 cycles, all the wires goes to a thermo-mechanical stabilization process; this is in agreement with the trend of the parameters reported in the Figures 8 and 9.
A second result is visible in the stable condition (at 1000$^{th}$ cycle). Considering the length of the NiTi wire and the working frequency of the damper, it can be seen that at a fixed working frequency, the temperature cycle oscillates around a minimum value that decreases with the length of the NiTi wire (Figure 15); besides, at a fixed length of the NiTi wire, the temperature cycle oscillates around a minimum value that increases with the working frequency (see Table 2). Additionally, the difference between the temperature of the short and long wires (delta values of Table 2) decreases with frequency. It means that with the increasing of frequency the short and the long wires reach almost the same temperature at the equilibrium, even if they go through a different path of phase transformation.

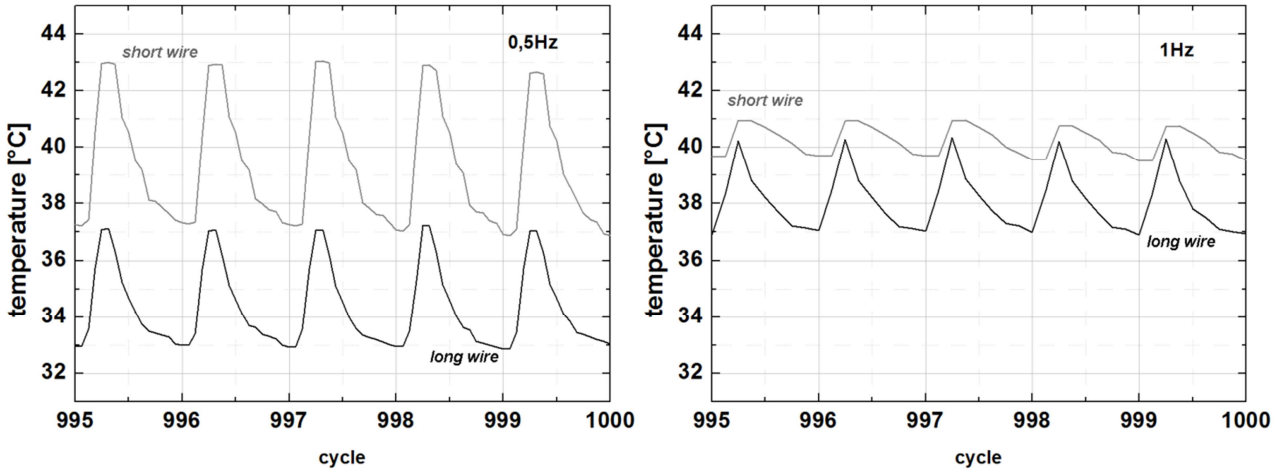


Figure 15. Temperature of the short and long wires of the damper during the last five mechanical cycles at 0.5 and 1Hz.

| working frequency of the damper [Hz] | minimum temperature of the short NiTi wire [℃] | minimum temperature of the long NiTi wire [℃] | delta [℃] |
|---|---|---|---|
| **0.5** | 37 | 33 | 5 |
| **1** | 39.5 | 37 | 2.5 |

Table 2. Minimum temperature at stable conditions of short and long NiTi wires as a function of the working frequency of the damper.

Some further comments arise by considering the temperature change $\Delta T$ of the NiTi wire during the loading and the unloading paths (see Figure 16 for a generic mechanical cycle). First, it has to take in mind that the NiTi wires have a particular working mode: in accordance to what reported in Figure 4, each NiTi wire is in the loading path for a period that is four times lower than the working period of the damper (T). Therefore, each wire gets warm in a period lower than that employed to cool down (unloading time together with the rest time, see Figure 4). Figures 17 and 18 show that the temperature cycle appears asymmetric at the beginning of the mechanical tests; in fact, in the first $50^{th}$ cycles, the temperature change $\Delta T$ registered during the loading path is higher than that registered during the unloading period (cooling and rest periods). After the $50^{th}$ mechanical cycle, this feature is no longer valuable as $\Delta T$ upon loading is the same as that registered during unloading; consequently, in stable condition the temperature cycle becomes symmetric independently by both the NiTi wires length and the working frequency of the damper.

Furthermore, one can also notice that at 0.5Hz, $\Delta T$ of the short wire is higher than that of the long one because of the different strains. On the contrary, at 1Hz the temperature change of the short wire is lower than that of the long wire. It means that at high strains (i.e. the case of the short wire in this paper) and at a frequency near 1Hz, there is a change of the normal and expected functioning of the NiTi wire. In fact, this results is somewhat in contradiction with the Clausius-Clapeyron law, according to which the increase of the stress happens with a simultaneous increase of temperature. This point is now into consideration, and new experiments are currently in course.

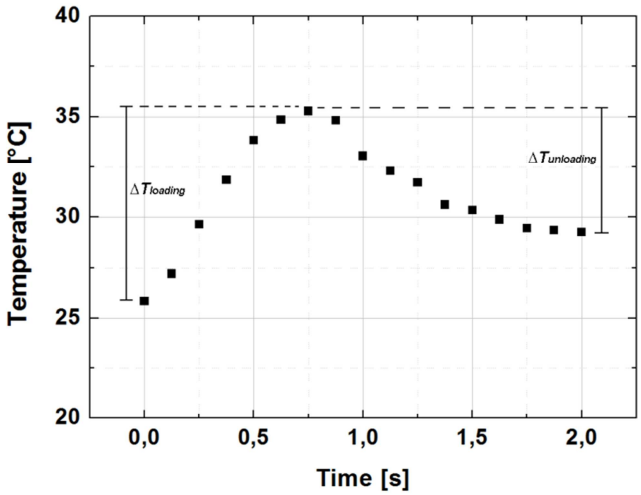


Figure 16.Temperature cycle of a NiTi wire with the indication of the temperature change of the NiTi wire during the loading and the unloading paths, $\Delta T_{loading}$ and $\Delta T_{unloading}$. Unloading also accounts for the rest period.

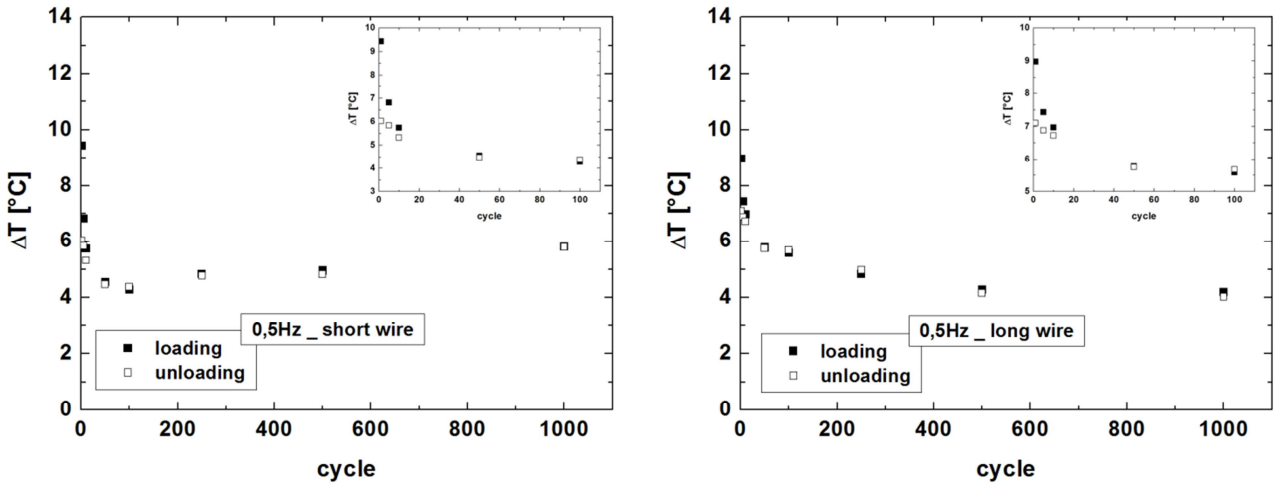


Figure 17. Amplitude of the temperature cycle during the loading and the unloading paths, at 0.5Hz. A detailed view of the first 100 cycles is reported in the insets.

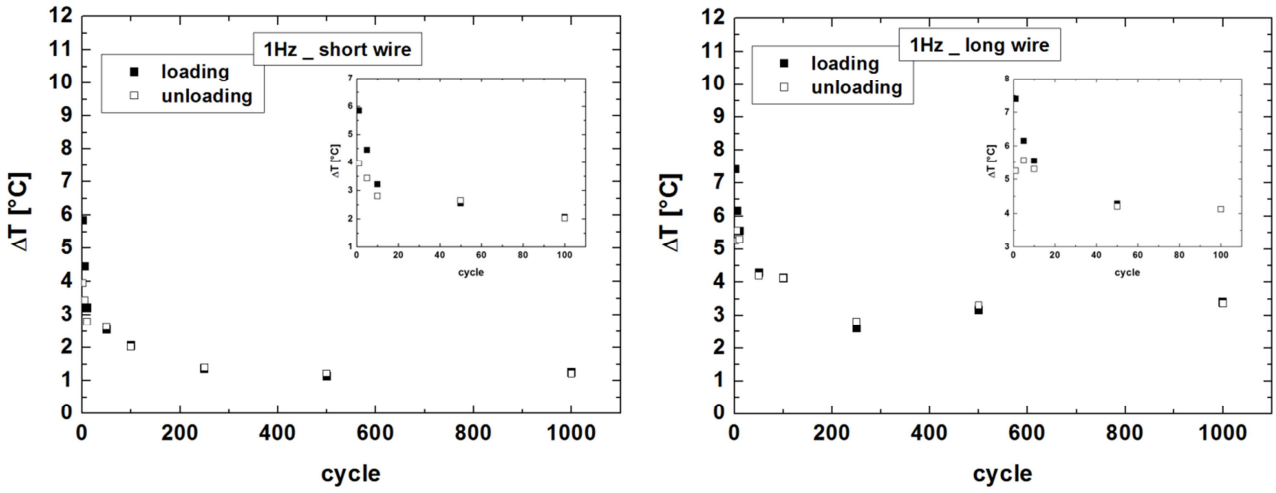


Figure 18. Amplitude of the temperature cycle during the loading and the unloading paths, at 1Hz. A detailed view of the first 100 cycles is reported in the insets.

## Conclusions

A new pseudoelastic damper composed by NiTi wires with different length has been tested following requirements typical of seismic events: frequencies of 0.5, 1 and 2Hz and 1000 mechanical cycles were considered. It was found that in the first 50 cycles, the device goes through a stabilization process of the main energetic parameters. Furthermore, frequency affects the damping performance by altering the hysteretic shape of the mechanical response of the damper with consequential thermal effects that allows the increasing of the loads. It was found that the proposed damper assures a bi-directional motion throughout the 1000 cycles together with the preservation of the recentering. Additionally, some interesting thermal effects were also observed: at high frequency and at high strains the maximum force increases but the temperature of the NiTi wire decreases being in contraddiction with the Clausius-Clapeyron law.

## Aknowledgements

Authors are gratefull to Dr. Dario Ripamonti for the precious technical assistance and for the helpful and constructive discussions throughout all measurements.

**References**


[1] Otsuka K and Ren X Physical metallurgy of Ti–Ni-basedshape memory alloys Prog. Mater. Sci. 50 511–6782005

[2] Nespoli A, Rigamonti D, Riva M, Villa E, Passaretti F, Study of pseudoelastic systems for thedesign of complex passive dampers: staticanalysis and modeling. Smart Mater. Struct. 25 (2016) 105001

[3] Chen QF, Zuo XB, Wang LM, Chang W, Tian WY, Li AQ, Yang H, Liu LH. NiTi wire as a superelastic damping material in structural engineering, Mater. Sci. Eng. A A 438-440 (2006) 1089-1092

[4] Yam MCH, Fang C, Lam ACC, Zhang Y, Numerical study and practical design of beam-to-column connections with shape memory alloys. J. constr. steel Res. 104 (2015) 177-192

[5] Menna C, Auricchio F, Asprone D. Applications of shape memory alloys in structural engineering, Shape memory alloys Engineering ISBN 978-0-08-099920-3 Elsevier Ltd. 2015 369-403

[6] Parulekar YM, reddy GR, Vaze KK, Guha S, Gupta C, Muthumani K, Sreekala R. Seismic response attenuation of structures using shape memory alloy dampers, Struct. Control Health Monit. 2012 19:102-119

[7] Torra V, Isalgue, Lovey FC, Sade M, Shape memory alloys as an effective tool to damp oscillations. Study of the fundamental parameters required to guarantee technological applications. J. Therm. Anal. Calorim (2015) 119:1475-1533

[8] Huang B, Zhang H, Wang H, Song G, Passive base isolation with superelastic nitinol SMA helical springs. Smart Mater. Struct. 23 (2014) 065009

[9] Qian H, Li H, Song G, Experimental investigations of building structure with a superelastic shape memory alloy friction damper subject to seismic loads. Smart Mater. Struct. 25 (2016) 125026

[10] Qian H, Li H, Song G, Guo W, Recentering Shape Memory Alloy Passive Damper for Structural Vibration Control. Mathematical Problems in Engineering, vol. 2013, Article ID 963530, 13 pages, 2013. doi:10.1155/2013/963530

[11] Branco M, Gonçalves A, Guerreiro L, Ferreira J, Cyclic behavior of composite timber-masonry wall in quasi-dynamic conditions reinforced with superelastic damper. Construction and Building Materials 52 (2014) 166–176

[12] Parulekar YM, Reddy GR, Vaze KK, Guha S, Gupta C, Muthumani K, Sreekala R, Seismic response attenuation of structures using shape memory alloy dampers. Struct. Control Health Monit., 19: 102–119. doi:10.1002/stc.428

[13] Fang C, Yam MCH, Lam ACC, Xie L, Cyclic performance of extended end-plate connections equipped with shape memory alloy bolts. Journal of Constructional Steel Research 94 (2014) 122–136
[14] Rofooei FR, Farhidzadeh FR, Investigation on The Seismic Behavior of Steel MRF with Shape Memory Alloy Equipped Connections. Procedia Engineering 14 (2011) 3325–3330
[15] Kuang Y, Ou J, Passive smart self-repairing concrete beams by using shape memory alloy wires and fibers containing adhesives. J. Cent. South Univ. Technol. (2008) 15: 411417
[16] Dolce M, Cardone D, Marnetto R, Implementation and testing of passive control devices based on shape memory alloys. Earthquake Engng Struct. Dyn. 2000; 29: 945-968
[17] Nemat-Nasser S, Guo WG, Superelastic and cyclic response of NiTi SMA at variousstrain rates and temperatures, Mec. Mater. 38 (2006) 463–474
[18] Liu Y, Mahmud A., Kursawe F., Nam TH., Effect of pseudoelastic cycling on the Clausius–Clapeyron relation for stress-induced martensitic transformation in NiTi. J. Alloys Comp. 449 (2008) 82–87
[19] Schmidt I, Lammering R. The damping behaviour of superelastic NiTi components. Mater. Sci. Eng. A 378 (2004) 70-75
[20] He Y, Yin H, Zhou R, Sun Q, Ambient effect on damping peak of NiTi shape memory alloy, Mater. Letters 64 (2010) 1483-1486
[21] Khan Q, Yu C, Kang G, Li J, Yan W, Experimental observations on rate-dependent cyclic deformation of super-elastic NiTi shape memory alloy. Mech. Mater. 97 (2016) 48-58
[22] Shaw JA, Kiriakids S, Thermomechanical aspects of NiTi, J. Mech. Phys. Solids, 43 (1995) 1243-1281
[23] Soul H, Isalgue A, Yawny A, Torra V, Lovey FC. Pseudoelastic fatigue of NiTi wires: frequency and size effects on damping capacity. Smart. Mater. Struct. 19 (2010) 085006
[24] He YJ, Sun QP, Frequency-dependent temperature evolution in NiTi shape memory alloy under cyclic loading, Smart. Mater. Struct. 19 (2010) 115014
[25] Carfagni M, Lenzi E and Pierini M 1998 The loss factor as ameasure of mechanical damping Conf.: 1998 IMAC XVI—16th Int. Modal Analysis Conf. pp 580–4
[26] Wang X, Xu B, Yue Z, Phase transformation behavior of pseudoelastic NiTi shape memory alloys under large strain, J. Alloys Comp. 463 (2008) 417-422
[27] Maletta C, Sgambitterra E, Furgiuele F, Casati R, Tuissi A, Fatigue properties of a pseudoelastic NiTi alloy: Strain ratcheting and hysteresis under cyclic tensile loading, International Journal of Fatigue 66 (2014) 78–85
[28] Mao S, Han X, Wu MH, Zhang Z, Hao F, Liu D, Zhang Y, Hou B, Effect of cyclic loading on apparent Young's modulus and critical stress in nano-subgrained superelastic NiTi shape memory alloys. Mater. Trans. 47 (2006) 735-741

[29] Bonnot E, Romero R, Manosa L, Vives E, Planes A, Elastocaloric effect associated with the martensitic transition in shape memory alloys, Phys. Reviw Letters 2008
[30] Ossmer H, Miyazaki S, Kohl M, Elastocaloric heat pumping using a shape memory alloy foil device,2015 Transducers - 2015 18th International Conference onSolid-State Sensors, Actuators and Microsystems (TRANSDUCERS)